Punjab University
Journal of Mathematics (ISSN 1016-2526)
Vol. 51(2)(2019) pp. 91-104

# Decay of a Potential Vortex. Fractional Model

Muhammad Ans Nazar
Abdus Salam School of Mathematical Sciences,
Government College University, Lahore, Pakistan.
Email: ansnazar7@gmail.com

Constantin Fetecau
Academy of Romanian Scientists,
Bucharest 050094, Romania.
Email: c_fetecau@yahoo.com

Received: 16 February, 2018 / Accepted: 25 April, 2018 / Published online: 16 December, 2018

**Abstract.** Decay of a potential vortex through an incompressible viscous fluid is numerically studied using a fractional model. The influence of temporal and spatial fractional parameters on the fluid velocity and the circulation on a circle of radius *r* is graphically represented and discussed. As the corresponding diagrams are almost identical and difficult enough to be distinguished, five tables with numerical values have been included. The differences are small enough, but they exist. In all cases the vortex deaden in space. As a check of results that have been obtained, a comparison between numerical and exact solutions is presented. As expected, when the fractional parameters are in close proximity of one and the third parameter $\delta$ tends to one, the velocity profiles corresponding to the numerical solution tends to superpose over that of exact solution.

**AMS (MOS) Subject Classification Codes: 35S29; 40S70; 25U09**
**Key Words:** Potential vortex, Viscous fluid, Fractional model.

## 1. Introduction

The decay problem of a potential vortex through a viscous fluid was analytically and graphically solved by Zierep [19]. It consists in the following initial value problem

$$\frac{\partial \omega(r,t)}{\partial t} = \nu \left( \frac{\partial^2}{\partial r^2} + \frac{1}{r}\frac{\partial}{\partial r} - \frac{1}{r^2} \right) \omega(r,t);\ \ r,t>0 \text{ and } \omega(r,0) = \frac{\Gamma_0}{2\pi r}, \tag{1. 1}$$

where $\omega(r,t)$ is the rotational component of velocity in the cylindrical coordinate system $(r,\theta,z)$, $\nu$ is the kinematic viscosity of the fluid and $\Gamma_0$ is the circulation of the potential vortex. The corresponding solution that has been obtained by means of the similarity transformation of variables has the simple form

$$\omega(r,t) = \frac{\Gamma_0}{2\pi r}\left\{1 - exp\left(-\frac{r^2}{4\nu t}\right)\right\}. \tag{1. 2}$$

The value of the circulation $\Gamma(r,t)$ on a circle of radius $r$, which is of physical interest because it describes the diffusion of vorticity, is

$$\Gamma(r,t) = 2\pi r\omega(r,t) = \Gamma_0\left\{1 - exp\left(-\frac{r^2}{4\nu t}\right)\right\}. \tag{1. 3}$$

The solution of this interesting problem has been already extended to second grade [10], Maxwell [8] and Oldroyd-B [9] fluids. In all cases, the classical solutions (1.2) and (1.3) have been recovered as limiting cases of the corresponding solutions. The decay of the potential vortex and of the corresponding tangential shear stress in such fluids have been graphically underlined and discussed and comparisons with viscous fluids have been also provided. Unfortunately, the usage of fractional derivatives in the governing equations of Newtonian fluids has been never taken into consideration although the interest for fractional models has been substantially increased in the last time.

Fractional calculus gained importance and popularity due to its vast potential of applications in various fields including rheology, quantum mechanics, heat transfer, polymer physics, chemical physics and many others. The first authors who applied fractional derivatives in viscoelasticity are Bagley and Torvik [2] and a very good agreement with experimental results using fractional calculus has been obtained by Caputo and Mainardy [5, 6]. It seems that the fractional differential equations accurately describe different physical phenomena than the corresponding ordinary partial differential equations and the first authors who used a time fractional derivative in the governing equation of a viscous fluid were Debnath and Bhatta [7]. Recently, Pan et al. [15] used the spatial fractional derivative in the temperature equation and found it more capable to explain the abnormal thermal conductivity enhancement as compared with the integer order derivative.

On the other hand, the fractional models are more adequate because the fractional order derivatives can describe memory and hereditary properties of materials [14]. Furthermore, Makris et al. [13] used experimental data in order to calibrate a fractional derivative Maxwell model. More exactly, they found the value of the fractional parameter so that the predicted material properties to be in excellent agreement with the experimental data. In the existing literature, there are more definitions of the fractional derivative and two of them have been recently used by Abro et al. [1] and Raza [17]. In order to see them, as well as for an interesting review concerning the applications and the importance of fractional calculus, we recommend the work of Sheoran and Kundu [18].

Based on the above-mentioned observations, our interest here is to study the decay of a potential vortex through a viscous fluid using a fractional model. Particularly, we want to know how the two fractional parameters (temporal and spatial) affect this potential vortex. For this, the dimensionless fractional partial differential equation governing the motion is numerically solved by means of the finite difference method. The influence of fractional parameters on the decay of potential vortex and the circulation $\Gamma(r,t)$ is graphically underlined and discussed and comparisons with the classical solutions (1.2) and (1.3) are also included. However, in order to bring to light all hypotheses under which the classical solution (1.2) exists, we determined it by means of the integral transform method.

## 2. Statement of the Problem

In the following, we consider the partial differential equation $(1.1)_1$ with the initial distribution of velocity

$$\omega(r,0)=\frac{\Gamma_\delta}{2\pi r^\delta};\quad \delta\in(0,1]. \tag{2. 4}$$

The new initial condition is a generalization of the condition $(1.1)_2$. It allows us to enlarge $(\delta>1)$ or to diminish $(\delta<1)$ the vortex intensity.

In order to provide solutions that are free of the flow geometry, we introduce the next non-dimensional entities

$$t^*=\frac{t}{t_0},\ r^*=\frac{r}{(\Gamma_\delta t_0)^{\frac{1}{\delta+1}}},\ \omega^*=\frac{2\pi\omega}{(\frac{\Gamma_\delta}{t_0^\delta})^{\frac{1}{\delta+1}}},\ \Gamma^*=\frac{\Gamma}{(\Gamma_\delta^2 t_0^{1-\delta})^{\frac{1}{1+\delta}}},\ \nu_\delta=\frac{\nu}{(\Gamma_\delta^2 t_0^{1-\delta})^{\frac{1}{1+\delta}}}, \tag{2. 5}$$

where $t_0$ is a characteristic time and the dimension of the constant $\Gamma_\delta$ is $\frac{m^{1+\delta}}{s}$. It reduces to $\Gamma_0$ for $\delta=1$. Introducing Eqs. (2.5) in (1.1) and (2.4) and dropping out the star notation, it results that

$$\frac{\partial\omega(r,t)}{\partial t}=\nu_\delta\left(\frac{\partial^2}{\partial r^2}+\frac{1}{r}\frac{\partial}{\partial r}-\frac{1}{r^2}\right)\omega(r,t),\ r,t>0;\ \omega(r,0)=\frac{1}{r^\delta}. \tag{2. 6}$$

As regards the circulation $\Gamma(r,t)$, its non-dimensional form is

$$\Gamma(r,t)=r\omega(r,t). \tag{2. 7}$$

The dimensionless fractional model corresponding to this problem is based on the fractional partial differential equation

$$D_t^\alpha\omega(r,t)=\nu_\delta\left(D_r^{2\beta}+\frac{1}{r}D_r^\beta-\frac{1}{r^2}\right)\omega(r,t);\ r,t>0, \tag{2. 8}$$

with the initial condition $(2.6)_2$. Here $D_t^\alpha(.)$ and $D_r^\beta(.)$, $D_r^{2\beta}(.)$ are temporal, respectively spatial Caputo fractional derivatives which are defined by [3].

$$D_u^\epsilon f(u)=\begin{cases}\frac{1}{\Gamma(n-\epsilon)}\int_0^u\frac{f^{(n)}(v)}{(u-v)^{1+\epsilon-n}}dv & n\in N\setminus\{0\},\ n-1<\epsilon<n,\\ f^{(n)}(u) & n\in N.\end{cases} \tag{2. 9}$$

According to this definition, in order to determine the value of a time fractional derivative in a given point, all previous values of the respective function have to be taken into consideration. Consequently, the memory formalism which is a characteristic of the behavior of viescoelastic fluids can be represented using fractional derivatives.

## 3. NUMERICAL SOLUTION

In order to solve the fractional partial derivative equation (2.8) with the initial condition $(2.6)_2$, we firstly make the transformation $s = t^{\alpha}$ and search for a series solution of the form

$$\omega(r,s) = \sum_{m=0}^{\infty} a_m(r) s^m = a_0(r) + a_1(r)s + a_2(r)s^2 + ... \tag{3. 10}$$

Replacing Eq. (3.10) in (2.8) and using the identity

$$D_t^{\alpha} s^m = D_t^{\alpha} t^{m\alpha} = \frac{\Gamma(1+m\alpha)}{\Gamma(1+m\alpha-\alpha)} t^{m\alpha-\alpha} = \frac{\Gamma(1+m\alpha)}{\Gamma\left(1+(m-1)\alpha\right)} s^{m-1};\ m \geq 1, \tag{3. 11}$$

we obtain

$$\begin{aligned}\sum_{m=1}^{\infty} a_m(r) b_m^{-1} s^{m-1} &= \nu \sum_{m=0}^{\infty} \left[ D_r^{2\beta} a_m(r) + \frac{1}{r} D_r^{\beta} a_m(r) - \frac{1}{r^2} a_m(r) \right] s^m \\ &= \nu \sum_{m=1}^{\infty} \left[ D_r^{2\beta} a_{m-1}(r) + \frac{1}{r} D_r^{\beta} a_{m-1}(r) - \frac{1}{r^2} a_{m-1}(r) \right] s^{m-1},\end{aligned} \tag{3. 12}$$

where $b_m = \frac{\Gamma[1+(m-1)\alpha]}{\Gamma(1+m\alpha)}$.

Identifying the coefficients of $s^{m-1}$, we find the recurrence relation

$$a_m(r) = \nu b_m \left[ D_r^{2\beta} a_{m-1}(r) + \frac{1}{r} D_r^{\beta} a_{m-1}(r) - \frac{1}{r^2} a_{m-1}(r) \right];\ m \geq 1, \tag{3. 13}$$

with (see Eqs. $(2.6)_2$ and (3.10))

$$a_0(r) = \omega(r,o) = \frac{1}{r^{\delta}}. \tag{3. 14}$$

In order to determine the solution of the recurrent equation (3.13), we shall use the finite difference method for different intervals of the fractional parameter $\beta$.

**Case 1:** $0 < \beta < \frac{1}{2}$

On the interval [0,R] we consider the grid points $0 = r_0 < r_1 < r_2 < ... < r_n = R;\ r_n = nh,\ h = \frac{R}{N},\ n = 0,1,2,...,N$

In this case both $\beta$ and $2\beta$ belong to (0,1) and the Caputo derivative of a function $f(r)$ in the point $r_n$ is given by

$$D_r^{\epsilon} f(r_n) = \frac{1}{\Gamma(1-\epsilon)} \int_0^{r_n} \frac{f'(\rho)}{(r_n-\rho)^{\epsilon}} d\rho = \frac{1}{\Gamma(1-\epsilon)} \sum_{j=1}^{n} \int_{r_{j-1}}^{r_j} \frac{f'(\rho)}{(r_n-\rho)^{\epsilon}} d\rho. \tag{3. 15}$$

For $\rho \in [r_{j-1}, r_j]$ the value of the derivative $f'(\rho)$ can be approximated by $\frac{f(r_j)-f(r_{j-1})}{h}$. Consequently, Eq. (3.15) becomes

$$\begin{aligned} D_r^{\epsilon} f(r_n) &= \frac{1}{\Gamma(1-\epsilon)} \sum_{j=1}^{n} \frac{f(r_j)-f(r_{j-1})}{h} \int_{r_{j-1}}^{r_j} \frac{1}{(r_n-\rho)^{\epsilon}} d\rho \\ &= \sum_{j=1}^{n} \gamma_{nj} [f(r_j) - f(r_{j-1})]; \quad n = 1, 2, ..., N, \end{aligned} \tag{3. 16}$$

where

$$\gamma_{nj} = \frac{1}{h\Gamma(2-\epsilon)} \left[ (r_n - r_{j-1})^{1-\epsilon} - (r_n - r_j)^{1-\epsilon} \right]. \tag{3. 17}$$

According to the last two equalities, we can write that

$$D_r^{2\beta} a_{m-1}(r_n) = \sum_{j=1}^{n} c_{nj} \left[ a_{m-1}(r_j) - a_{m-1}(r_{j-1}) \right] = A_{m-1,n}, \tag{3. 18}$$

$$D_r^{\beta} a_{m-1}(r_n) = \sum_{j=1}^{n} d_{nj} \left[ a_{m-1}(r_j) - a_{m-1}(r_{j-1}) \right] = B_{m-1,n}, \tag{3. 19}$$

where $n = 1, 2, 3, ..., N$, $m = 1, 2, 3, ...$ and

$$\begin{aligned} c_{nj} &= \frac{1}{h\Gamma(2-2\beta)} [(r_n - r_{j-1})^{1-2\beta} - (r_n - r_j)^{1-2\beta}], \\ d_{nj} &= \frac{1}{h\Gamma(2-\beta)} [(r_n - r_{j-1})^{1-\beta} - (r_n - r_j)^{1-\beta}]. \end{aligned} \tag{3. 20}$$

Using Eqs. (3.18) and (3.19) in Eq. (3.13), we find that

$$a_{m,n} = \nu b_m (A_{m-1,n} + r_n^{-1} B_{m-1,n} - r_n^{-2} a_{m-1,n}); \; n = 1, 2, ..., N, \; m = 1, 2, 3, ... \tag{3. 21}$$

where $a_{m,n} = a_m(r_n)$. Consequently, the solution of the fractional partial derivative equation (2.8) in the grid points $\{r_n\}$ is given by

$$\omega(r_n, t) = \sum_{m=0}^{\infty} a_m(r_n) s^m = \sum_{m=0}^{\infty} a_{m,n} t^{\alpha m}; \; n = 1, 2, ..., N, \; m = 1, 2, 3, ... \tag{3. 22}$$

where the coefficients $a_{m,n}$ are determined by the recurrent equation (3.21).

**Case 2:** $\frac{1}{2} < \beta \leq 1$

In this case $1 < 2\beta \leq 2$ and, according to the definition (2.9),

$$D_r^{2\beta} a_{m-1}(r) = \frac{1}{\Gamma(2-2\beta)} \int_0^r \frac{a''_{m-1}(\rho)}{(r-\rho)^{2\beta-1}} d\rho. \tag{3. 23}$$

On the interval $[r_{j-1}, r_j]$ the second order derivative $a''_{m-1}(\rho)$ can be approximated by the relation

$$a''_{m-1}(\rho) \approx \frac{a_{m-1}(r_{j+1}) - 2a_{m-1}(r_j) + a_{m-1}(r_{j-1})}{h^2}; \;\; j - 1, 2, ..., n, \; m = 1, 2, 3, ... \tag{3. 24}$$

and the Caputo derivative $D_r^{2\beta} a_{m-1}(r)$ in the grid point $r_n$ is given by

$$D_r^{2\beta} a_{m-1}(r_n) = \sum_{j=1}^{n} \frac{a_{m-1}(r_{j+1}) - 2a_{m-1}(r_j) + a_{m-1}(r_{j-1})}{h^2\Gamma(3-2\beta)} \times \\ [(r_n - r_{j-1})^{2-2\beta} - (r_n - r_j)^{2-2\beta}] = C_{m-1,n}. \tag{3. 25}$$

The Caputo derivative $D_r^{\beta} a_{m-1}(r_n)$ is approximated by the same equality (3.19) and the approximate solution of our equation (2.8) is again given by Eq. (3.22) with

$$a_{m,n} = \nu b_m (C_{m-1,n} + r_n^{-1} B_{m-1,n} - r_n^{-2} a_{m-1,n});\ n = 1, 2, ..., N,\ m = 1, 2, 3, ... \tag{3. 26}$$

**Case 3:** $\beta = \frac{1}{2}$

In this case $2\beta = 1$ and the equality (3.13), in $r_n$, becomes

$$a_m(r_n) = \nu b_m [a'_{m-1}(r_n) + \frac{1}{r_n} D_r^{\frac{1}{2}} a_{m-1}(r_n) - \frac{1}{r_n^2} a_{m-1}(r_n)];\ m \geq 1. \tag{3. 27}$$

Direct computations show that $D_r^{\frac{1}{2}} a_{m-1}(r_n)$ can be approximated by

$$D_r^{\frac{1}{2}} a_{m-1}(r_n) \approx 2 \sum_{j=1}^{n} \frac{a_{m-1}(r_j) - a_{m-1}(r_{j-1})}{h\sqrt{\pi}} [(r_n - r_{j-1})^{\frac{1}{2}} - (r_n - r_j)^{\frac{1}{2}}] = D_{m-1,n}. \tag{3. 28}$$

while

$$a'_{m-1}(r_n) \approx \frac{a_{m-1,n} - a_{m-1,n-1}}{h} = E_{m-1,n}. \tag{3. 29}$$

Introducing Eqs. (3.28) and (3.29) in (3.27), it results that

$$a_{m,n} = \nu b_m (E_{m-1,n} + r_n^{-1} D_{m-1,n} - r_n^{-2} a_{m-1,n}). \tag{3. 30}$$

## 4. Exact solution for $\alpha = \beta = 1$, $\delta = 1$

It is worth pointing out the fact that our numerical solutions from the previous section are not conclusive without any comparison with an exact solution. Such a solution, as it results from introduction, has been provided by Zierep without any proof. He used the similarity by transformation of variables but did not present the hypotheses (restrictive conditions) under which this solution exists. In order to bring to light these conditions, and to avoid repetition, we shall determine this solution using the Hankel transform. To do that, in addition to the natural conditions

$$\omega(r,t),\ \frac{\partial\omega(r,t)}{\partial r} \to 0\ as\ r \to \infty, \tag{4. 31}$$

the following supplementary hypotheses

$$\lim_{r\to 0} r\omega(r,t) = 0,\ \lim_{r\to\infty} r\omega(r,t) < \infty,\ \lim_{r\to 0} r\frac{\partial\omega(r,t)}{\partial r} < \infty,\ \lim_{r\to\infty} r\frac{\partial\omega(r,t)}{\partial r} < \infty, \tag{4. 32}$$

have to be imposed. The two conditions from Eq. (4.31) assure the fact that the fluid is quiescent at infinity and there is no shear in the free streems [4, 16].

Now, multiplying Eq. $(2.6)_1$ by $rJ_1(\rho r)$ and integrating with respect to $r$ from 0 to infinity, we find that

$$\frac{\partial\omega_H(\rho,t)}{\partial t}=\nu\int_0^\infty rJ_1(\rho r)\left(\frac{\partial^2}{\partial r^2}+\frac{1}{r}\frac{\partial}{\partial r}-\frac{1}{r^2}\right)\omega(r,t)dr, \tag{4. 33}$$

where $J_1(.)$ is the standard Bessel function of first kind and order one, and

$$\omega_H(\rho,t)=\int_0^\infty r\omega(r,t)J_1(\rho r)dr, \tag{4. 34}$$

is the Hankel transform of $\omega(r,t)$.

Direct computations clearly show that, in the view of previous conditions (4.31) and (4.32), the integral from Eq. (4.33) reduces to (see also [7])

$$\int_0^\infty rJ_1(\rho r)\left(\frac{\partial^2}{\partial r^2}+\frac{1}{r}\frac{\partial}{\partial r}-\frac{1}{r^2}\right)\omega(r,t)dr=-\rho^2\omega_H(\rho,t). \tag{4. 35}$$

Introducing Eq. (4.35) in (4.33) and bearing in mind the initial condition $(2.6)_2$ with $\delta=1$ and the fact that the Hankel transform of $\frac{1}{r}$ is $\frac{1}{\rho}$, we attain to the next initial value problem

$$\frac{\partial\omega_H(\rho,t)}{\partial t}+\nu\rho^2\omega_H(\rho,t)=0;\ \omega_H(\rho,0)=\frac{1}{\rho}, \tag{4. 36}$$

whose solution is given by

$$\omega_H(\rho,t)=\frac{1}{\rho}e^{-\nu\rho^2 t};\ t>0. \tag{4. 37}$$

Finally, applying the inverse Hankel transform to Eq. (4.37) and using the known result [12].

$$\int_0^\infty J_1(\rho r)e^{-a^2\rho}d\rho=\frac{1}{r}\left\{1-exp\left(-\frac{r^2}{4a^2}\right)\right\}, \tag{4. 38}$$

we find

$$\omega(r,t)=\frac{1}{r}\left\{1-exp\left(-\frac{r^2}{4\nu t}\right)\right\}, \tag{4. 39}$$

which is just the dimensionless form of the classical solution (1.2). Introducing Eq. (4.39) in (2.7), the corresponding dimensionless form of the circulation $\Gamma(r,t)$ is

$$\Gamma(r,t)=1-exp\left(-\frac{r^2}{4\nu t}\right). \tag{4. 40}$$

## 5. Numerical results and discussions

Exact solutions for the velocity $\omega(r,t)$ and the circulation $\Gamma(r,t)$ corresponding to the decay of a potential vortex through a viscous fluid, with or without time fractional derivative, have been developed and discussed by Fetecau et al. [11], respectively Zierep [19]. The purpose of this work is to extend the previous results to a fractional model with temporal and spatial fractional derivatives. Moreover, in order to obtain a larger variation of the vortex magnitude, the initial distribution of velocity was taken under the form (2.4). Due to the computing difficulties, as well as of the intricate form of an exact solution, the problem is numerically solved using a software based on the finite difference method. In the classical case, when $\alpha = \beta = \delta = 1$, the exact solution is determined using Hankel transform in order to bring to light all restrictions in which this solution exists.

Now, in order to see the influence of fractional parameters $\alpha$ and $\beta$ on the dimensionless velocity $\omega(r,t)$ and the corresponding circulation $\Gamma(r,t)$, their profiles are depicted in Figs. 1-5 for $\delta = 0.25$ or 0.5 and different values of $\alpha$ and $\beta$. Since these profiles are very close and difficult to be distinguished, the tables 1-5 containing the exact values of the two physical entities have been added. Finally, in order to emphasize the accuracy of numerical solutions that have been here obtained, the diagrams of $\omega(r,t)$ and $\Gamma(r,t)$ are presented for the different values of $\delta \to 1$ and $\alpha = \beta = 0.95$ (nearby to one) in Fig. 6. In all figures $\nu = 0.003$ (air), $\Gamma_0 = 4$ and $t_0 = 3$ in SI units.

In Figs. 1 and 2 the diagrams of velocity and circulation against *r* are displayed at three values of $\alpha$, two values of $\delta$ and fixed values of *t* and $\beta \in \left(0, \frac{1}{2}\right)$. The diagrams of the two physical entities seem to be almost identical for all values of *r*, but the difference between their values appears in Tables 1 and 2. Approximately speaking, in all cases the fluid velocity smoothly decreases from maximum values in the vicinity of $r = 0$ to the zero value for large values of *r* while the circulation increases from the zero value to the asymptotic value for *r* going to infinity. The influence of $\delta$, as it results from the two tables, is significant. In addition, as expected, the values of velocity and circulation are higher for $\delta = 0.5$ as compared to those corresponding to $\delta = 0.25$. Consequently, the vortex intensity decreases for decreasing values of $\delta$. In the case of $\delta = 0.25$ and $\alpha = 0.45$ or 0.65 the fluid velocity increases for low values of *r* and then decreases to the asymptotic value.

Figs. 3 and 4 present similar diagrams when the temporal fractional parameter $\alpha$ is fixed and $\beta$ varies between 0 and $\frac{1}{2}$ and the results are almost identical both as form and intensity. Fig. 5 presents the diagrams of velocity and circulation when $\alpha$ varies between (0,1) and $\beta = 0.95$ is greater than 1/2. In this case, their profiles have the same form as those of classical solutions for all values of $\alpha$ but seem to be identical. This is the reason that we included here the table 5.

In the last figure 6, the profiles of $\omega(r,t)$ and $\Gamma(r,t)$ against *r* are presented both for ordinary and fractional fluids when $\alpha = \beta = 0.95$ (very close to one) and $\delta$ going to one. As expected, the velocity diagrams are almost identical as form to those obtained by Zierep [19, Fig. 7] and Fetecau et al. [11, Fig. 1]. More exactly, in all cases, the fluid velocity increases up to a maximum value in the proximity of $r = 0$ and then smoothly decreases to the zero value for increasing values of *r*. Consequently, the vortex intensity diminishes for increasing values of *r* and the vortex deaden in space. Furthermore, when $\delta \to 1$, the velocity profiles tend to superpose over that corresponding to the ordinary case. As regards the circulation $\Gamma(r,t)$, as well as in [11, Fig.2], it smoothly increases from zero value to the asymptotic value 1.

| | Velocity $\omega(r,t)$ | | | Circulation $\Gamma(r,t)$ | | |
|---|---|---|---|---|---|---|
| | $\beta = 0.45$ | | | $\beta = 0.45$ | | |
| $r$ | $\alpha = 0.45$ | $\alpha = 0.65$ | $\alpha = 0.85$ | $\alpha = 0.45$ | $\alpha = 0.65$ | $\alpha = 0.85$ |
| 0.015 | 2.15961 | 2.21563 | 2.29752 | 0.03224 | 0.03323 | 0.03446 |
| 0.03 | 2.22382 | 2.24535 | 2.26954 | 0.0667 | 0.06736 | 0.06809 |
| 0.045 | 2.0965 | 2.10641 | 2.11692 | 0.09434 | 0.09479 | 0.09526 |
| 0.06 | 1.98118 | 1.98654 | 1.99215 | 0.11887 | 0.11919 | 0.11953 |
| 0.075 | 1.88711 | 1.89039 | 1.89381 | 0.14153 | 0.14178 | 0.14204 |
| 0.09 | 1.81003 | 1.81222 | 1.81448 | 0.1629 | 0.1631 | 0.1633 |
| 0.105 | 1.74567 | 1.74722 | 1.74881 | 0.1833 | 0.18346 | 0.18363 |
| 0.12 | 1.69091 | 1.69205 | 1.69323 | 0.20291 | 0.20305 | 0.20319 |
| 0.135 | 1.64354 | 1.64441 | 1.64531 | 0.22188 | 0.222 | 0.22212 |
| 0.15 | 1.60199 | 1.60267 | 1.60338 | 0.2403 | 0.2404 | 0.24051 |

Table 1: Dimensionless velocity and circulation values corresponding to Fig. 2.1 for different values of *r*

| | Velocity $\omega(r,t)$ | | | Circulation $\Gamma(r,t)$ | | |
|---|---|---|---|---|---|---|
| | $\beta = 0.45$ | | | $\beta = 0.45$ | | |
| $r$ | $\alpha = 0.45$ | $\alpha = 0.65$ | $\alpha = 0.85$ | $\alpha = 0.45$ | $\alpha = 0.65$ | $\alpha = 0.85$ |
| 0.015 | 5.63885 | 5.84042 | 6.10644 | 0.08458 | 0.08761 | 0.0916 |
| 0.03 | 5.19504 | 5.26196 | 5.33712 | 0.15585 | 0.15786 | 0.16011 |
| 0.045 | 4.49051 | 4.51921 | 4.55007 | 0.20207 | 0.20336 | 0.20475 |
| 0.06 | 3.97095 | 3.9858 | 4.00151 | 0.23826 | 0.23915 | 0.24009 |
| 0.075 | 3.5868 | 3.59557 | 3.60476 | 0.26901 | 0.26967 | 0.27036 |
| 0.09 | 3.29196 | 3.29762 | 3.30354 | 0.29628 | 0.29679 | 0.29732 |
| 0.105 | 3.05773 | 3.06163 | 3.06569 | 0.32106 | 0.32147 | 0.3219 |
| 0.12 | 2.86633 | 2.86915 | 2.87209 | 0.34396 | 03443 | 0.34465 |
| 0.135 | 2.70636 | 2.70848 | 2.71068 | 0.36536 | 0.36564 | 0.36594 |
| 0.15 | 2.57017 | 2.57181 | 2.57351 | 0.38553 | 0.38577 | 0.38603 |

Table 2: Dimensionless velocity and circulation values corresponding to Fig. 2.2 for different values of *r*

| | Velocity $\omega(r,t)$ | | | Circulation $\Gamma(r,t)$ | | |
|---|---|---|---|---|---|---|
| | $\alpha = 0.65$ | | | $\alpha = 0.65$ | | |
| $r$ | $\beta = 0.10$ | $\beta = 0.30$ | $\beta = 0.50$ | $\beta = 0.10$ | $\beta = 0.30$ | $\beta = 0.10$ |
| 0.015 | 2.15725 | 2.17911 | 2.20052 | 0.03236 | 0.03269 | 0.03301 |
| 0.03 | 2.23585 | 2.24123 | 2.24418 | 0.06708 | 0.06724 | 0.06733 |
| 0.045 | 2.10353 | 2.10567 | 2.10637 | 0.09466 | 0.09476 | 0.09479 |
| 0.06 | 1.98544 | 1.98652 | 1.98668 | 0.11913 | 0.11919 | 0.1192 |
| 0.75 | 1.88998 | 1.89058 | 1.89057 | 0.14175 | 0.14179 | 0.14179 |
| 0.09 | 1.81212 | 1.81247 | 1.81238 | 0.16309 | 0.16312 | 0.16311 |
| 0.105 | 1.74728 | 1.74749 | 1.74737 | 0.18346 | 0.18349 | 0.18347 |
| 0.12 | 1.69219 | 1.69232 | 1.69219 | 0.20306 | 0.202308 | 0.20306 |
| 0.135 | 1.6446 | 1.64467 | 1.64454 | 0.22202 | 0.22203 | 0.22201 |
| 0.15 | 1.60289 | 1.60292 | 1.60279 | 0.24043 | 0.24044 | 0.24042 |

Table 3: Dimensionless velocity and circulation values corresponding to Fig. 2.3 for different values of *r*

| | Velocity $\omega(r,t)$ | | | Circulation $\Gamma(r,t)$ | | |
|---|---|---|---|---|---|---|
| | $\alpha = 0.65$ | | | $\alpha = 0.65$ | | |
| *r* | $\beta = 0.10$ | $\beta = 0.30$ | $\beta = 0.40$ | $\beta = 0.10$ | $\beta = 0.30$ | $\beta = 0.40$ |
| 0.015 | 5.64259 | 5.7164 | 5.78902 | 0.08464 | 0.08575 | 0.08684 |
| 0.03 | 5.24415 | 5.25754 | 5.26216 | 0.15732 | 0.15773 | 0.15786 |
| 0.045 | 4.51819 | 4.52193 | 4.52117 | 0.20332 | 0.20349 | 0.20345 |
| 0.06 | 3.98755 | 3.98874 | 3.98742 | 0.23925 | 0.23932 | 0.23925 |
| 0.075 | 3.59781 | 3.59808 | 3.59681 | 0.26984 | 0.26986 | 0.26976 |
| 0.09 | 3.29983 | 3.29971 | 3.2986 | 0.29698 | 0.29697 | 0.29687 |
| 0.105 | 3.06376 | 3.06337 | 3.06241 | 0.32169 | 0.32165 | 0.32155 |
| 0.12 | 2.871 | 2.87062 | 2.86979 | 0.34452 | 0.34447 | 0.34438 |
| 0.315 | 2.71015 | 2.70973 | 2.70901 | 0.36587 | 0.36581 | 0.36572 |
| 0.15 | 2.57332 | 2.5729 | 2.57226 | 0.386 | 0.38593 | 0.38584 |

Table 4: Dimensionless velocity and circulation values corresponding to Fig. 2.4 for different values of *r*

| | Velocity $\omega(r,t)$ | | | Circulation $\Gamma(r,t)$ | | |
|---|---|---|---|---|---|---|
| | $\beta = 0.95$ | | | $\beta = 0.95$ | | |
| *r* | $\alpha = 0.45$ | $\alpha = 0.65$ | $\alpha = 0.85$ | $\alpha = 0.45$ | $\alpha = 0.65$ | $\alpha = 0.85$ |
| 0.015 | 1.84312 | 1.89217 | 1.96663 | 0.02765 | 0.02838 | 0.0295 |
| 0.03 | 2.00281 | 2.04255 | 2.09158 | 0.06008 | 0.06128 | 0.06275 |
| 0.045 | 1.97881 | 2.00315 | 2.03006 | 0.08905 | 0.09014 | 0.09135 |
| 0.06 | 1.91084 | 1.92547 | 1.9409 | 0.11465 | 0.11553 | 0.11645 |
| 0.075 | 1.83983 | 1.84917 | 1.85895 | 0.13799 | 0.13869 | 0.13942 |
| 0.09 | 1.77533 | 1.78175 | 1.78852 | 0.15978 | 0.16036 | 0.16097 |
| 0.105 | 1.71857 | 1.72327 | 1.72828 | 0.18045 | 0.18094 | 0.18147 |
| 0.12 | 1.6688 | 1.67241 | 1.6763 | 0.20026 | 0.20069 | 0.20116 |
| 0.135 | 1.62491 | 1.6278 | 1.63094 | 0.21936 | 0.21975 | 0.22018 |
| 0.15 | 1.58592 | 1.58829 | 1.59089 | 0.23789 | 0.23824 | 0.23863 |

Table 5: Dimensionless velocity and circulation values corresponding to Fig. 2.5 for different values of *r*

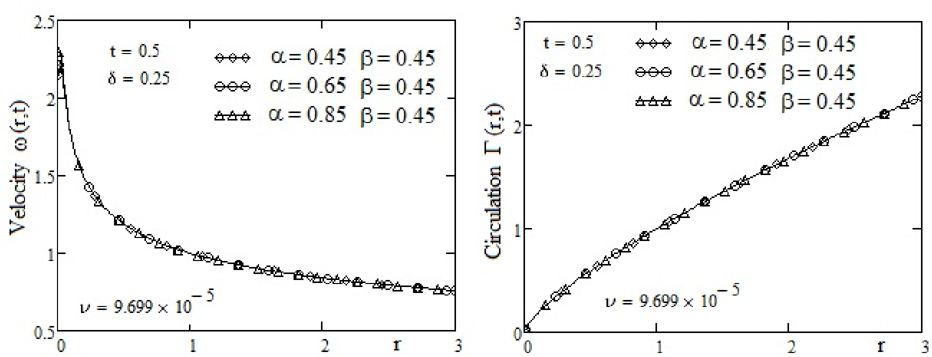


FIGURE 1. Velocity and circulation profiles against *r* for fractional model when $\delta = 0.25$, $\beta = 0.45 < \frac{1}{2}$ and different values of $\alpha$

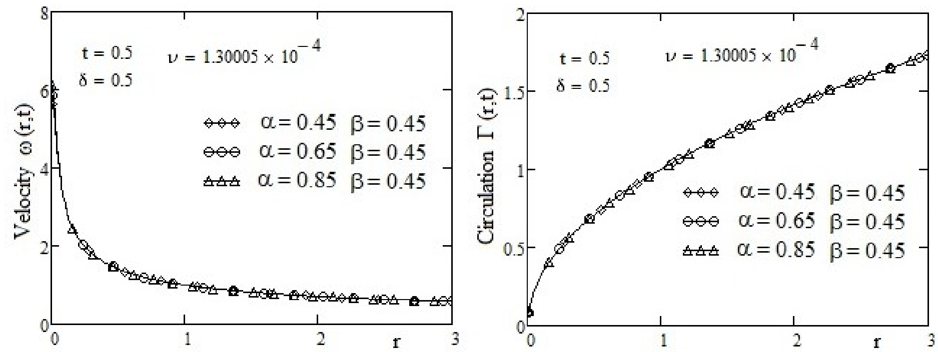


FIGURE 2. Velocity and circulation profiles against $r$ for fractional model when $\delta = 0.5$, $\beta = 0.45 < \frac{1}{2}$ and different values of $\alpha$

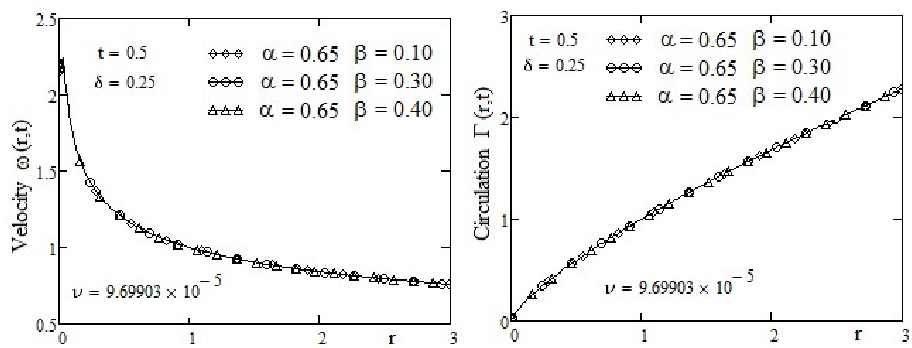


FIGURE 3. Velocity and circulation profiles against $r$ for fractional model when $\delta = 0.25$, $\alpha = 0.65$ and different values of $\beta < \frac{1}{2}$

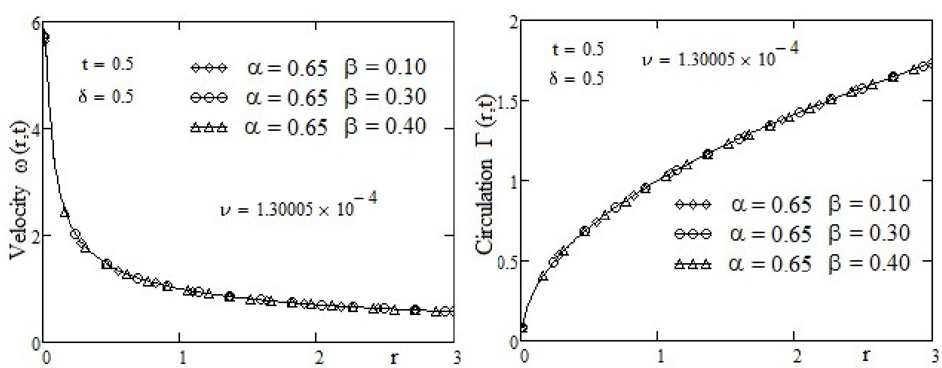


FIGURE 4. Velocity and circulation profiles against $r$ for fractional model when $\delta = 0.5$, $\alpha = 0.65$ and different values of $\beta < \frac{1}{2}$

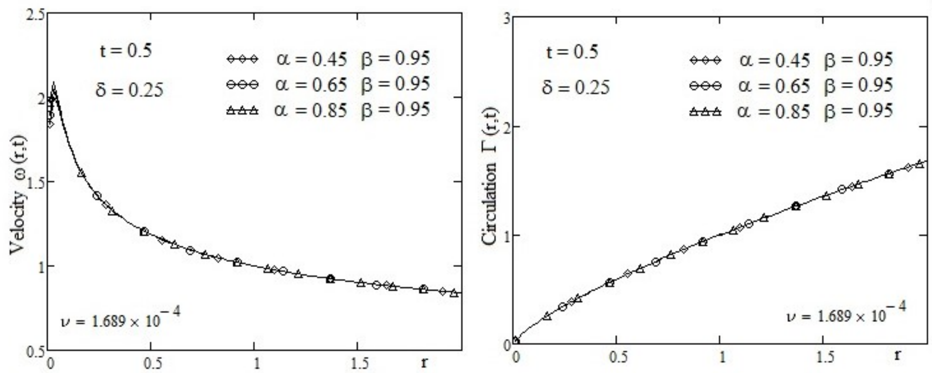


FIGURE 5. Velocity and circulation profiles against *r* for fractional model when $\delta = 0.25$, $\beta = 0.95 > \frac{1}{2}$ and different values of $\alpha$

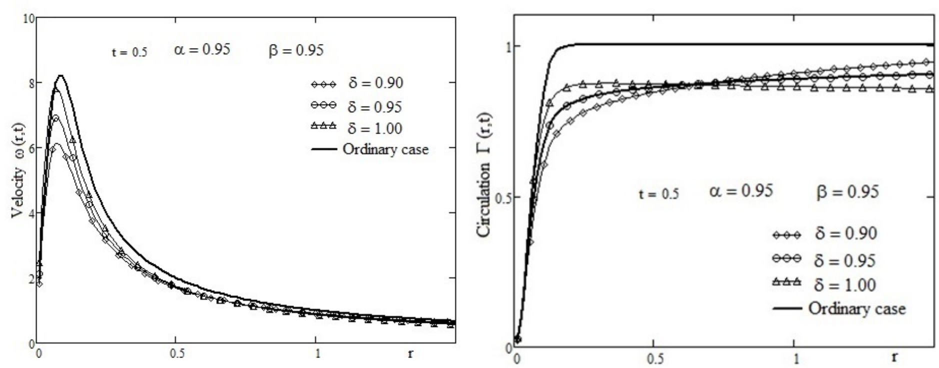


FIGURE 6. Velocity and circulation profiles against *r* for ordinary and fractional models at different values of $\delta$

## 6. CONCLUSION

The decay of a potential vortex in a Newtonian fluid is numerically studied using a fractional model with temporal and spatial fractional derivatives. To allow a larger variation of the vortex magnitude, the initial distribution of velocity has been a little changed. The employment of fractional parameters allow us to get a larger scale of values of the solutions in which the memory effects are taken into consideration. Furthermore, there exists the possibility to determine the values of fractional parameters so that the predicted characteristics of the model to be in excellent agreement with the exact data corresponding to those of a real vortex. The intensity or the force of vortex can be also extended or diminished by means of the initial condition $(2.6)_2$.

In order to bring to light the influence of fractional parameters on the vortex, the profiles of velocity $\omega(r,t)$ and the circulation $\Gamma(r,t)$ are presented in Figs. 1-5 for two different initial conditions ($\delta = 0.25$ and 0.5) and diverse values of $\alpha$ and $\beta$. As these profiles are difficult to be distinguished, five tables with exact values are included. The close values of the magnitude of the two relevant physical entities at fixed values of $\alpha$ and $\beta$ but different values of *r* justify the proximity of their diagrams. In Fig. 6, for comparison, the diagrams of the same entities are presented both for ordinary and fractional model for values of $\alpha$ and $\beta$ closed to one and $\delta$ going to one. The main conclusions can be summarized as:

- In all cases the fluid velocity increases until a maximum value in the vicinity of $r = 0$ and then smoothly decreases to the zero value for large values of *r*.
- The circulation $\Gamma(r,t)$ smoothly increases from zero value to the asymptotic value 1.
- Fluid velocity, as well as the circulation, is an increasing function with respect to the fractional parameters $\alpha$ and $\beta$ if $\delta < 1$ . Consequently, as expected, the vortex intensity is lower for fractional in comparison to ordinary fluids. An opposite effect appears when $\delta > 1$ but the corresponding graphs are not included here.
- For $\alpha = \beta = 0.95$ (around one) and $\delta$ going to one, as it was to be expected, the profiles of velocity and circulation tend to superpose over those corresponding to ordinary fluids.

## Figure Legends

Fig. 1. Velocity and circulation profiles against *r* for fractional model when $\delta = 0.25$. $\beta = 0.45 < 1/2$ and different values of $\alpha$.

Fig. 2. Velocity and circulation profiles against *r* for fractional model when $\delta = 0.25$, $\beta = 0.45 < 1/2$ and different values of $\alpha$.

FIg. 3. Velocity and circulation profiles against *r* for fractional model when $\delta = 0.25$, $\alpha = 0.65$ and different values of $\beta < 1/2$.

Fig. 4. Velocity and circulation profiles against *r* for fractional model when $\delta = 0.5$, $\alpha = 0.65$ and different values of $\beta < 1/2$.

Fig. 5. Velocity and circulation profiles against *r* for fractional model when $\delta = 0.25$, $\beta = 0.95 > 1/2$ and different values of $\alpha$.

Fig. 6. Velocity and circulation profiles against *r* for ordinary and fractional models at different values of $\delta$.

## 7. Acknowledgments

The The author Muhammad Ans Nazar is highly thankful to the Abdus Salam School of Mathematical Sciences, GC University, Lahore and Higher Education Commission of Pakistan for generous supporting and facilitating his research work.

## REFERENCES


[1] K. A. Abro and M. A. Solangi, *Heat Transfer in Magnetohydrodynamic Second Grade Fluid with Porous Impacts using Caputo-Fabrizio Fractional Derivatives*, Punjab Univ. j. math **49**, No. 2 (2017) 113-125.

[2] R. L. Bagley and P. J. Torvik, *A theoretical basis for the application of fractional calculus to viscoelasticity*, J. Rheol. **27**, (1983) 201-210.

[3] D. Baleanu, B. Agheli and M. M. A. Qurashi, *Fractional advection differential equation within Caputo and Caputo-Fabrizio derivatives*, Adv. Mech. Eng. **8**, (2016) 1-8.

[4] R. Bandelli, K. R. Rajagopal and G. P. Galdi, *On some unsteady motions of fluids of second grade*, Arch. Mech. **47**, (1995) 661-676.

[5] M. Caputo and F. Mainardi, *A new dissipation model based on memory mechanism*, Pure Appl. Geophys, **91**, (1971) 134-147.

[6] M. Caputo and F. Mainardi, *Linear models of dissipation in anelastic solids*, Riv. Nuovo Cimento **1**, (1971) 161-198.

[7] L. Debnath and D. Bhatta, *Integral Transforms and Their Applications*, Second. Ed. Chapman and Hall/CRC Press, Boca-Raton, 2007.

[8] C. Fetecau and C. Fetecau, *Decay of a potential vortex in a Maxwell fluid*, Int. J. Non-Linear Mech. **38**, (2003) 985-990.

[9] C. Fetecau and C. Fetecau, *Decay of a potential vortex in an Oldroyd-B fluid*, Int. J. Eng. Sci. **43**, (2005) 340-351.

[10] C. Fetecau, C. Fetecau and J. Zierep, *Decay of a potential vortex and propagation of a heat wave in a second grade fluid*, Int. J. Non-Linear Mech. **37**, (2002) 1051-1056.

[11] C. Fetecau, D. Vieru and A. T. Ahmed, *Time fractional Oseen problem for viscous fluids*, Ann. Acad. Rom. Sci. Ser. Math. Appl. **10**, No. 1 (2018) 165-178.

[12] I. S. Gradshteyn and I. M. Ryzhik, *Alay Jeffery (Ed.), Tables of Integrals, Series and Products, fifth ed.* Academic Press, San Diego, New York, Boston, London, Sydney, Toronto, 1994 (translated from Russians).

[13] N. Makris, G. J. Dargush and M. C. Constantinou, *Dynamic analysis of generalized viscoelastic fluids*, J. Eng. Mech. **119**, (1993) 1663-1679.

[14] I. Podlubny, *Fractional Differential Equations*, Academic Press, New York, 1999.

[15] M. Pan, L. Zheng, F. Liu and X. Zhang, *Modeling heat transport in nanofluids with stagnation point flow using fractional calculus*, Appl. Math. Model. **40**, (2016) 8974-8984.

[16] K. R. Rajagopal and A. S. Gupta, *An exact solution for the flow of a non-Newtonian fluid past an infinite porous plate*, Meccanica **19**, (1984) 1948-1953.

[17] N. Raza, *Unsteady Rotational Flow of a Second Grade Fluid with Non-Integer Caputo Time Fractional Derivative*, Punjab Univ. j. math **49**, No. 3 (2017) 15-25.

[18] S. S. Sheoran and P. Kundu, *Fractional order generalized thermoelasticity theories: A review*, Int. J. Adv. Appl. Math. and Mech. **3**, (2016) 76-81.

[19] J. Zierep, *Similarity Laws and Modeling*, Marcel Dekker, Inc. New York, 1971.